



# Monitoring the drought in Southern Africa from space-borne GNSS-R and SMAP data

Komi Edokossi<sup>1</sup> · Shuanggen Jin<sup>1,2</sup> · Usman Mazhar<sup>1</sup> · Iñigo Molina<sup>1,3</sup> · Andres Calabia<sup>4</sup> · Irfan Ullah<sup>5,6</sup>

Received: 19 April 2022 / Accepted: 3 March 2024 / Published online: 28 March 2024  
© The Author(s), under exclusive licence to Springer Nature B.V. 2024

## Abstract

Drought, a highly detrimental natural disaster, poses significant threats to both human populations, wildlife, and vegetation. Traditional methods of monitoring soil moisture levels rely on ground-based measurements from meteorological stations. However, these stations often lack comprehensive coverage in certain agricultural areas, necessitating the use of alternative methods such as satellite remote sensing. This technique provides a reliable means of measuring soil moisture, a critical factor in effective agricultural management. This paper investigates variations in soil moisture and drought using data from the Cyclone Global Navigation Satellite System (CYGNSS) and the Soil Moisture Active and Passive (SMAP) system. To evaluate the accuracy of these data products, we compared both datasets with the Global Land Data Assimilation System (GLDAS) NOAH model from 2018 to 2019. Our findings reveal a strong correlation between the datasets and the model, with Pearson correlation coefficients ( $r$ ) and Root Mean Square Errors (RMSE) of approximately  $r=0.98$  and  $RMSE=0.03$  for SMAP, and  $r=0.97$  and  $RMSE=0.02$  for CYGNSS, respectively. We further compared these measurement datasets with drought indicators such as the Standardized Precipitation Index over three months (SPI3), the Normalized Difference Vegetation Index (NDVI), and Total Water Storage (TWS). The correlation coefficients between SMAP and the three indicators (NDVI, SPI3, and TWS) were 0.93, 0.84, and 0.047, respectively, while the coefficients between CYGNSS and the same indicators were 0.86, 0.78, and 0.56, respectively. All the variables also exhibited significant  $p$ -values. Despite minor differences, the results demonstrate excellent agreement. Our findings underscore the sensitivity of space-based sensors to drought conditions, highlighting their effectiveness as tools for detecting and monitoring drought (e.g. agricultural drought), particularly in the short term.

**Keyword** Soil moisture · Drought · Remote sensing · SPI3 · NDVI · TWS

## 1 Introduction

Drought, a formidable natural disaster, can wreak havoc on human populations, wildlife, and vegetation. In the agricultural sector, it can lead to a decrease in crop yield and livestock (Parry 2007), while in forestry, it can stunt tree growth and escalate the incidence of wildfires (Field 2012). These effects can precipitate economic and financial challenges, particularly in low-income countries (Godfray et al. 2010). Over recent decades, severe droughts in East Africa (2010–2011) and Southern Africa (1994–1995, 2015–2016, 2018–2019) have inflicted substantial damage on societies and ecosystems (Seager et al. 2015). Consequently, the monitoring and prediction of droughts can help alleviate their impacts by providing early warnings and contributing significantly to regional water resource management and economic development.

Traditional drought monitoring methods encompass ground-based measurements or grid interpolations of soil moisture from meteorological and agricultural perspectives (Sheffield et al. 2012). However, many agricultural areas lack meteorological stations, and even where these stations exist, their numbers are often insufficient to provide reliable spatiotemporal variability data (Easterling 2013). Moreover, data from different observation stations may not share the same record extents or data quality, complicating drought analysis (AghaKouchak et al. 2012).

Fortunately, satellite remote sensing has made significant strides in drought monitoring in recent years. This method enables the observation of hydrological variables such as precipitation (Sorooshian et al. 2011), soil moisture (Entekhabi et al. 2004), evapotranspiration (Anderson et al. 2011b), Total Water Storage (TWS) (AghaKouchak et al. 2015), groundwater storage (Rodell et al. 2002), and snow (Kongoli et al. 2012), among others.

Satellite remote sensing, especially with microwave technology (SMOS: Soil Moisture and Ocean Salinity and SMAP: Soil Moisture Active and Passive) and the recently developed Cyclone Global Navigation Satellite System (CYGNSS), is a potent tool for tracking changes in soil moisture. This parameter is crucial for modeling biophysical processes, and its accurate monitoring can enhance rainfall estimation for flood forecasting (Brocca et al. 2010; Koster et al. 2010), drought monitoring or prediction (Rahmani et al. 2016; Enenkel et al. 2016; Sánchez et al. 2016) landslide prediction (Brocca et al. 2012; Bitelli et al. 2012), and soil erosion prediction (Singh and Thompson 2016). As such, soil moisture appears to be the most appropriate variable for agricultural strategies, measuring factors such as soil moisture intensity, duration, and spatial extent. Indeed, agricultural drought results from inadequate moisture to support crop growth. The technique of soil moisture remote sensing gained prominence with the launch of the SMAP mission in 2015 (Entekhabi et al. 2010a). To produce data with relatively high spatial (3 km, 9 km, and 36 km) and temporal resolution (2–3 days), it combines high spatial resolution active radar and coarse-resolution, yet highly sensitive, passive radiometer observations (Entekhabi et al. 2010a).

Recently, Global Navigation Satellite System-Reflectometry (GNSS-R) has emerged as a promising tool for soil moisture monitoring. The United States (GPS NAVSTAR), Europe (Galileo), Russia (GLONASS), and China (BeiDou) are among the GNSS constellations targeting navigation, positioning, and time synchronization (Hofmann-Wellenhof et al. 2008). GNSS-R measures their reflected signals on Earth's surface, which are used in estimating geophysical parameters such as soil moisture, although the current GNSS-R missions were originally designed for ocean altitudes, winds, and tropical cyclone observations (Jia et al. 2017). The UK Disaster Monitoring Constellation (UK-DMC) mission was

the first to carry GNSS-R in 2003 (Gleason et al. 2005), followed by the launch of Tech-DemoSat-1 in July 2014, the 3CAT-2 of the Polytechnic University of Catalonia (UPC) in August 2016, NASA's Cyclone GNSS (CYGNSS) in December 2016, and the GEROS (GNSS Reflectometry, Radio Occultation, and Scatterometry) experiment of the European Space Agency (ESA). The Bufeng-1 A and B satellites, whose mission targeted sea-surface wind monitoring, were successfully deployed in June 2019 (Wu et al. 2021a, b).

Numerous indices based on soil moisture have been developed, including the Standardized Soil Moisture Index (SSI) (Hao et al. 2013), the Soil Moisture Percentile (Sheffield et al. 2004), the Soil Water Index (SWI), the Soil Water Deficit Index (SWDI), and the Multivariate Soil Moisture Deficit Index (MSDI). Soil moisture can be derived either from Land Surface Model (LSM) simulations or from satellite measurement data. As noted by AghaKouchak (2014a), soil moisture is a vital variable for persistent drought monitoring. Satellite sensors for soil moisture include passive microwave (Njoku et al. 2003), active microwave (Takada et al. 2009), or a combination of both (Kim et al., 2012). The technique to estimate soil moisture utilizes the difference in permittivity between liquid water and dry soil. Microwave observations are limited to the top 2–5 cm of soil (Entekhabi et al., 2010a). However, for the root zone, a suitable LSM must be coupled with the microwave (Reichle et al. 2004). For further details on optical, thermal, passive, and active microwave soil moisture estimation, refer to Wang et al. (2009) or Edokossi et al. (2020), among others.

Recent studies have demonstrated the potential of SMAP data for large-scale soil moisture monitoring. For instance, Eswar et al. (2018) compared soil moisture from SMAP with modeled US Drought Monitor (UDM) and Standardized Precipitation Index (SPI) data. The results showed that SMAP observations accurately captured changes in drought intensity. Bai et al. (2018) estimated the Soil Water Deficit Index (SWDI) from SMAP for mainland China and demonstrated its effectiveness in detecting drought conditions. Agha-Kouchak et al. (2015) used Water Cycle Multi-Mission Observation Strategy (WACMOS) data to monitor drought in the Horn of Africa. Drought monitoring and prediction have been improved by integrating Advanced Microwave Scanning Radiometer-Earth Observing System (AMSR-E) data into real-time US Department of Agriculture International Production Assessment Division (USDA IPAD) soil models (Bolten et al. 2010). Furthermore, the Climate Change Initiative (CCI) can be used to monitor agricultural drought (Wagner et al. 2012). The CCI datasets can be combined with LSM to generate long-term reliable soil moisture products (Reichle et al. 2004).

The Standardized Precipitation Index (SPI) and the Standardized Precipitation Evapotranspiration Index (SPEI) are two indices developed for drought monitoring. The SPI, which ranges from SPI1 to SPI48, is based solely on precipitation and corresponds to different time scales of drought monitoring. Conversely, the SPEI considers both precipitation and evapotranspiration. This research focuses on the SPI (specifically SPI3) due to its established significance and broad applicability in drought monitoring. The SPEI, a relatively recent meteorological drought index introduced by Vicente-Serrano et al. (2010), is a multi-scalar index that includes the climatic water balance, i.e., the difference between precipitation and evapotranspiration, making it more sensitive to temperature changes (Beguería et al. 2014).

Recent scientific investigations have consistently highlighted the efficiency and relevance of SPI3 in the context of agricultural drought monitoring. These studies emphasize that SPI3 is particularly adept at capturing abrupt changes in precipitation patterns and their swift influence on drought conditions. It is generally agreed that short time scale SPI (1 to 3 months) may be associated with soil moisture and better describes agricultural

drought (Raziei et al. 2009; Vicente-Serrano et al. 2005). With the progressive development of drought propagation studies, the SPI3 and SPI6 indicators have been accepted for agricultural or hydrological drought studies due to the propagation of meteorological drought to agricultural or hydrological drought over a period of around 3 to 6 months (Forootan et al. 2019). It has been suggested that the SPI3 index is better suited for identifying drought events that ultimately affect agricultural practices (Gebrehiwot et al. 2011). Studies by Ji and Peters (2003) and Rossi and Niemeyer (2012) found that SPI3 is best correlated with vegetation response, making it ideal for identifying agricultural drought. Therefore, in this study, the SPI3 index has been chosen for comparisons with SMAP and CYGNSS soil moisture to evaluate their capability in drought monitoring.

This study aims at demonstrating the capability, reliability, and usefulness of the direct use of soil moisture data for drought monitoring in Southern Africa. We evaluate the capability and the efficiency of SMAP and CYGNSS moisture datasets for drought monitoring during 2018–2019. We employ the Global Land Data Assimilation System (GLDAS) model as a reference value for validation and detection of deviations or biases. Moreover, the spatiotemporal variations observed by SMAP and CYGNSS are compared to well-known drought indicators such as SPI3, NDVI, and TWS (LWE=Liquid Water Equivalence). The variability observed in soil moisture is analyzed to evaluate the performance in drought detection and monitoring. We compare the spatial distribution of SMAP and CYGNSS soil moisture data with the Southern Africa drought hotspots maps.

## 2 Data and methods

### 2.1 Study area

The Southern Africa region was chosen as the study area due to the recurring droughts that significantly impact the lives of its inhabitants. During 1994–1995, most Southern African countries experienced severe droughts. In the north-western part of Zimbabwe, the rainfall during the 1994–1995 season was among the lowest ever recorded. The 2015–2016 El Niño event resulted in life-threatening weather conditions in many countries. Recently, a similar situation was faced during 2018 to 2020 ([www.gdacs.org](http://www.gdacs.org)), and the concurrent availability of SMAP and CYGNSS data presents an unprecedented opportunity to investigate the geophysical processes during this drought period. Figure 1 displays the major vegetation biomes (Lawal et al. 2019) of the study area. An arid climate can be observed in the West, with less severity in the East. The limits of the humid climate are at approximately 20 degrees latitude South.

### 2.2 Data

Satellite Soil Moisture (SM) observations between 2018–2019, derived from the Soil Moisture Active and Passive (SMAP) and Cyclone Global Navigation Satellite System (CYGNSS), were utilized in this research. Other data such as the Standardized Precipitation Index over three months (SPI3), Normalized Difference Vegetation Index (NDVI), Total Water Storage (TWS) in Liquid Water Equivalent (LWE), soil moisture from the Global Land Data Assimilation System (GLDAS) Noah model, and rainfall data were also used.

The SMAP mission, launched by the National Aeronautics Space Agency (NASA) in January 2015, provides global measurements of soil moisture and freeze/thaw state

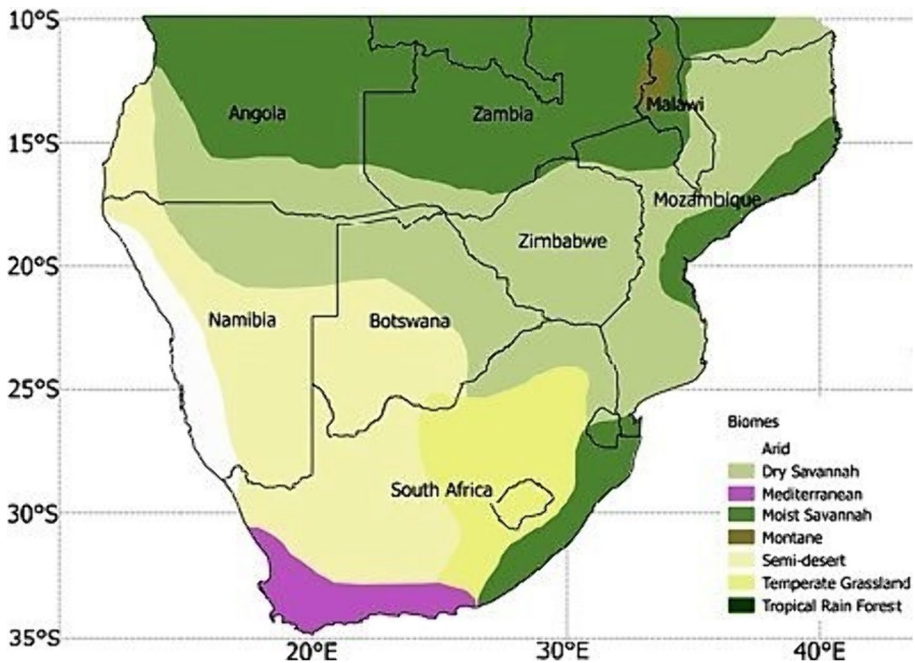


Fig. 1 Map of the study area with Major vegetation biomes (Lawal et al. 2019)

(Entekhabi et al. 2010a). The SMAP mission comprises both an L-band radar and an L-band radiometer, enabling global mapping of soil moisture at a 10 km spatial resolution with a 2–3 day revisit time under both clear and cloudy sky conditions. By integrating radiometer and radar measurements, SMAP provides high spatial resolution soil moisture data. The SMAP 10 km soil moisture data is obtained by combining higher accuracy but coarser spatial resolution (40 km) radiometer-based soil moisture retrieval with higher resolution radar data (1–3 km) that have lower retrieval accuracy. Moreover, the integration of these two types of data allows soil moisture to be estimated under a wider range of vegetation conditions (Entekhabi et al. 2010a). For SMAP data, we used the SMAP Enhanced L3 version 4 SM in this work (<https://nsidc.org/data/SPL3SMAP/versions/3>). The L3SMAP is a composite of daily estimates of global land surface conditions. The main parameter is surface soil moisture (approximately the top 5 cm on average in  $\text{cm}^3/\text{cm}^3$ ) presented on the global 9 km EASE-Grid 2.0 in Geotiff format.

The CYGNSS mission performs surface remote sensing with the target of measuring ocean surface wind under different weather conditions. It consists of 8 microsattellites with an average revisit time of seven hours and an inclination of  $35^\circ$  from the equator, which allows it to make measurements between approximately  $38^\circ$  N and  $38^\circ$  S latitude. For the CYGNSS data, we employed Level 3 version 1.0 soil moisture between 0–5 cm depth with a spatial resolution of  $0.3^\circ$  (Latitude)  $\times$   $0.37^\circ$  (Longitude) ([https://podaac.jpl.nasa.gov/dataset/CYGNSS\\_L3\\_SOIL\\_MOISTURE\\_V1.0](https://podaac.jpl.nasa.gov/dataset/CYGNSS_L3_SOIL_MOISTURE_V1.0)). The data are in volumetric water content ( $\text{cm}^3/\text{cm}^3$ ) and archived in daily files in netCDF-4 format.

The GLDAS model includes four land surface models: Mosaic, Noah, the Community Land Model (CLM), and the Variable Infiltration Capacity. The GLDAS soil moisture data is used as a reference value due to its accuracy and global coverage. In fact, GLDAS uses

advanced land surface modeling along with data assimilation techniques to provide optimal land surface states and fluxes. The monthly GLDAS Noah LSM L4 at  $0.25 \times 0.25^\circ$  resolution (version 2.1, GLDAS\_NOAH025\_M) is used to provide the top 10-cm soil moisture. This data product, reprocessed in January 2020, is obtained from the main production stream and it is a replacement for its previous version. The data is archived and distributed in NetCDF format. The GLDAS-2.1 products supersede their corresponding GLDAS-1 products ([https://disc.gsfc.nasa.gov/datasets/GLDAS\\_NOAH025\\_M\\_2.0/summary](https://disc.gsfc.nasa.gov/datasets/GLDAS_NOAH025_M_2.0/summary)).

Global Moderate Resolution Imaging Spectroradiometer (MODIS) vegetation indices are designed to provide consistent spatial and temporal comparisons of vegetation conditions. In this work, we used the global MOD13A3 monthly Normalized Difference Vegetation Index (NDVI), an ecological drought indicator, data at a 1-km spatial resolution as a gridded Level-3 product in the Sinusoidal projection (<https://modis.gsfc.nasa.gov/data/dataproduct/>).

The Standardized Precipitation Index (SPI) is an indicator of meteorological drought based solely on precipitation and can be utilized to study global agricultural droughts, hydrology, and ecosystem impact studies. SPI ranges from 1 to 48 months, corresponding to different precipitation accumulation periods (1, 3, 6, 9, ..., 48). SPI for short accumulation periods (SPI1 to SPI3) indicates immediate impacts such as soil moisture reduction. For this study, SPI3 was selected due to its wide recognition and utilization in the scientific community for agricultural drought study, its strong correlation with vegetation response, and the availability of the data for the entire study period. The SPI3 used in this study is generated by The International Research Institute (IRI/LDEO) Climate Data Library, University of Columbia (<https://iridl.ldeo.columbia.edu/>). The SPI3 values are the monthly precipitation at  $1.0^\circ$  latitude/longitude resolution calculated from a dataset that combines the retrospective and real-time CPC Gauge-OLR Blended (GOB) daily precipitation analysis for the globe, accumulated to monthly (<https://iridl.ldeo.columbia.edu/>).

Gravity Recovery and Climate Experiment (GRACE) and Follow-on (GRACE-FO) Total Water Storage (TWS) indices are considered as hydrological drought indicators, as these measure the change in water thickness near the Earth's surface. The GRACE mission was launched in March 2002 and provides temporal gravity field measurements with global coverage. The GRACE-FO mission was launched on May 21, 2018, with the primary goal to track Earth's mass movements and changes, particularly those related to water, with a key application in groundwater monitoring. Climate change exacerbation of drought conditions has increased dependence on groundwater for agricultural and other uses globally, thus its monitoring is required. The data used in this study is GRACE/GRACE-FO RL06 v02 Mascon Grids w/ Corrections Applied from the Center for Space Research (CSR) in Austin, Texas, USA. The data covers April 2002 to December 2022 and is in the NetCDF format ([https://www2.csr.utexas.edu/grace/RL06\\_mascons.html](https://www2.csr.utexas.edu/grace/RL06_mascons.html)).

We also employ rainfall data for comparison with soil moisture content variation. This dataset includes three products with different temporal resolutions: three-hourly (3B42), daily (3B42 derived), and monthly (3B43). The spatial resolution is  $0.25 \times 0.25^\circ$  and extends from latitude  $50^\circ$  S to  $50^\circ$  N. In this study, only the TRMM 3B43 product for 2018–2019 is used, which is the monthly mean of the TRMM 3B42 dataset ([https://disc.gsfc.nasa.gov/datasets/TRMM\\_3B43\\_7/summary](https://disc.gsfc.nasa.gov/datasets/TRMM_3B43_7/summary)).

## 2.3 Data analysis

The datasets utilized in this study (Table 1) were harmonized to a common spatial resolution, and the effects of the seasonal cycle were removed from the data to prevent

non-stationarity, which can lead to false correlations. The daily soil moisture from the SMAP and CYGNSS observations were converted into monthly samples. Given the inherent differences in spatial and temporal resolutions among the datasets used in this study, we employed the bilinear resampling method to standardize all datasets to a consistent 1° by 1° spatial resolution. This process was conducted within the R programming language. The bilinear resampling method calculates a pixel’s value based on a weighted distance average from its four adjacent pixels. Following this resampling process, we adjusted all datasets to a uniform monthly temporal resolution for further analysis, ensuring consistency and comparability across all datasets. The SMAP and CYGNSS soil moisture datasets were compared with the GLDAS soil moisture model, which was considered as reference data. We computed the Pearson correlation ( $r$ ) between the datasets using the overall average values. The Root Mean Square Errors (RMSE) were calculated to estimate the degree of performance and provide a reliable statistic to validate the agreement between datasets. Additionally, probability values ( $p$ -values) were computed to highlight the degree of significance in their correlations. The  $r$  and RMSE are calculated as follows:

$$r = \frac{\sum_{i=1}^n (X_i - \bar{X})(Y_i - \bar{Y})}{\sqrt{\sum_{i=1}^n (X_i - \bar{X})^2} \sqrt{\sum_{i=1}^n (Y_i - \bar{Y})^2}}$$

$$RMSE = \sqrt{\frac{\sum_{i=1}^n (Y_i - X_i)^2}{n}}$$

where,  $X_i$  and  $Y_i$  represent the GLDAS and SMAP or GLDAS and CYGNSS soil moisture data respectively, and  $\bar{X}$  and  $\bar{Y}$  are the mean value of the GLDAS with SMAP and GLDAS with CYGNSS data respectively, with  $n = 38$ .

### 3 Results

#### 3.1 Evaluation and validation of SMAP and CYGNSS soil moisture

To validate the SMAP and CYGNSS soil moisture data, soil moisture from 0 to 10 cm from GLDAS was used as a reference. Initially, scatter plots were generated between SMAP and GLDAS, and CYGNSS and GLDAS soil moistures. As depicted in Fig. 2, both soil moisture products exhibit a strong correlation with GLDAS soil moisture, with correlation coefficients ( $r$ ) of 0.76 and 0.83, respectively, and significant  $p$ -values of 0.06 and 0.05, respectively. Here,  $n=38$  represents the data points of the relationship between the SMAP and GLDAS, and between CYGNSS and GLDAS datasets. The points in scatterplot (b) are relatively closer to the trend line than those in scatterplot (a), illustrating a stronger correlation between them. A summary of the statistics is provided in Table 2.

Additionally, monthly soil moisture data from January 2018 to December 2019, derived from SMAP, CYGNSS, and GLDAS, were used to compute the time series plots (Fig. 3). In terms of correlation coefficient ( $r$ ) and Root Mean Square Error (RMSE), both SMAP and CYGNSS soil moisture performed well with GLDAS soil moisture, with  $r=0.98$  and  $RMSE=0.03$  for SMAP, and  $r=0.97$  and  $RMSE=0.02$  for CYGNSS, respectively. The low RMSE values indicate a good performance between the datasets. The variance is 0.78

**Table 1** Data used in the study

Sensors and products	Parameter	Drought type	Year	Spatial resolution	Temporal resolution
MOD13A3 (MODIS)	NDVI	Ecological drought	2018–2019	1 km	Monthly
L3SMAP-L-BAND RADIOMETER (SMAP)	Soil moisture	Agricultural drought	2018–2019	9 km	Daily
CYGNSS Level 3 (CYGNSS)	Soil moisture		2018–2019	$0.3^{\circ} \times 0.37^{\circ}$	1 day
GLDAS (NOAH model)	Soil moisture		2018–2019	$0.25^{\circ} \times 0.25^{\circ}$	Monthly
Climate Prediction Center's (CPC) Gauge-OLR Blended (GOB) SPI3	SPI3	Meteorological drought	2018–2019	$1.0^{\circ} \times 1.0^{\circ}$	3-Month
GRACE and GRACE-FO	TWS (LWE)	Hydrological drought	2018–2019	1 degree	Daily
TRMM (TMPA/3B43)	Rainfall	Meteorological drought	2018–2019	$0.25^{\circ} \times 0.25^{\circ}$	Monthly

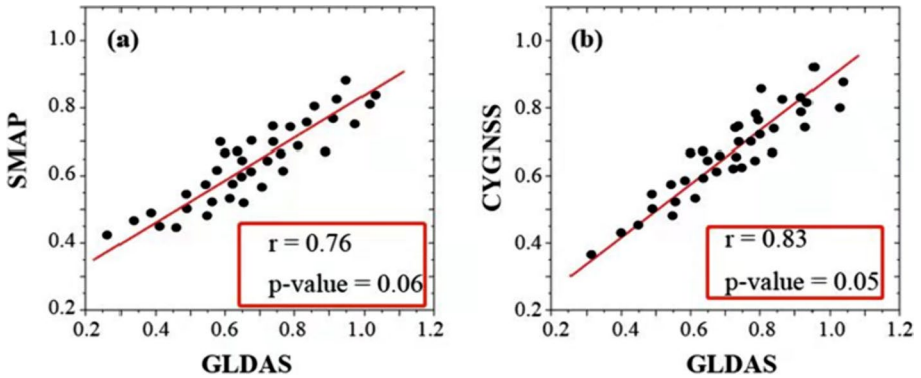


**Fig. 2** Scatter plot of SMAP and CYGNSS soil moisture with GLDAS soil moisture for 2018–2019. (The values reported in the figure are the average values of each variable of the two years)

**Table 2** Pearson correlation and *P*-values

	GLDAS soil moisture	SMAP soil moisture	CYGNSS soil moisture
Pearson’s <i>r</i>		0.76	0.83
<i>p</i> -values		0.06	0.05

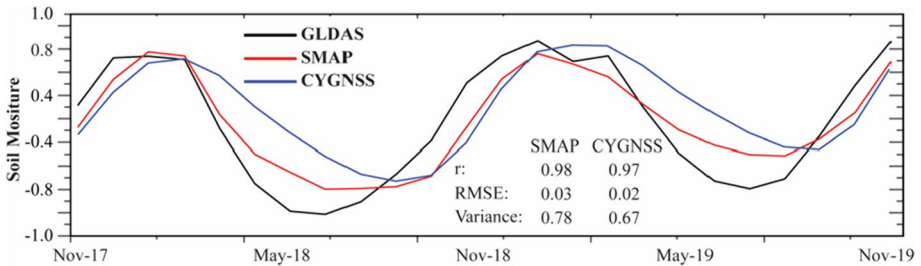


**Fig. 3** Time series plots of SMAP and CYGNSS soil moisture with GLDAS soil moisture for 2018 and 2019. (The values reported in the figure are the monthly value of each variable of the two years)

for SMAP and 0.67 for CYGNSS (Table 3). Furthermore, SMAP and CYGNSS soil moisture, along with GLDAS soil moisture on a monthly basis, show a good performance by capturing the features of GLDAS soil moisture (Fig. 3).

Whether in 2018 or 2019, GLDAS detected the drought first, followed by SMAP and CYGNSS. Moreover, SMAP and CYGNSS soil moisture values do not exhibit a net convex function as observed with GLDAS at the drought peak.

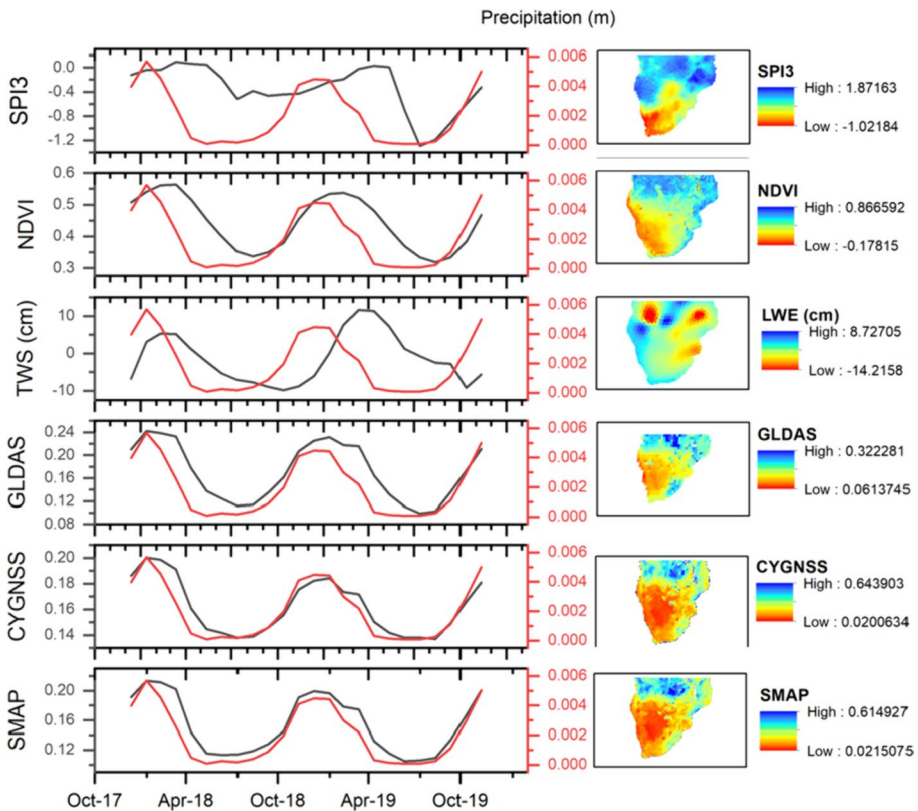
### 3.2 Time series plots of SMAP and CYGNSS soil moistures and drought indicators

Figure 4 illustrates the temporal evolution of the plots between SMAP and CYGNSS soil moisture and the drought indicators, compared with precipitation data for the period

**Table 3** Pearson correlation, variance and RMSE values for 2018–2019

2018–2019 GLDAS soil moisture			
SMAP soil moisture	Pearson’s r		0.98
	RMSE		0.03
	Variance		0.78
CYGNSS soil moisture	Pearson’s r		0.97
	RMSE		0.02
	Variance		0.67

2018–2019. The maps on the right side of the plots represent the spatial distribution maps of each variable for the same period. All the variables align well temporally on a global scale, with minor differences observed in the trend with SPI3 and TWS. In fact, SPI3 and TWS exhibit some shifts in the variations during the temporal evolution when compared against other variables. The dry and wet conditions monitored through SMAP and CYGNSS observations align well with the low and high value areas of the GLDAS and rainfall values, while SPI3 presents minor differences in the variation in the initial



**Fig. 4** Time series plot of SMAP and CYGNSS soil moisture, NDVI, TWS and SPI3 in comparison with precipitation data from January 2018 to December 2019. (The values reported in the maps are the average values of each variable of the two years, while the ones in the plots are the monthly value of each variable)

**Table 4** Correlation  $r$  and  $P$ -values between the variables

		SPI3	NDVI	TWS
SMAP soil moisture	Pearson's $r$	0.84	0.93	0.47
	$p$ -values	0.05	0.04	0.01
CYGNSS soil moisture	Pearson's $r$	0.78	0.86	0.56
	$p$ -values	0.04	0.03	0.02

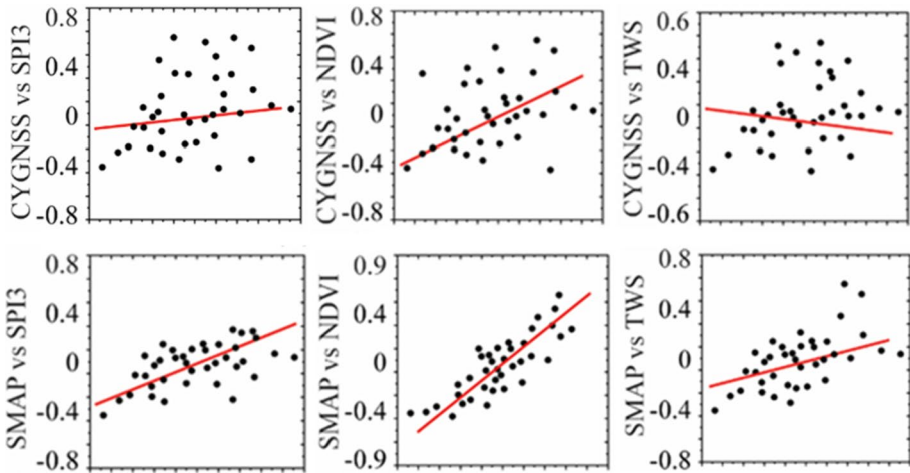


**Fig. 5** Scatter plots between soil moistures (SMAP and CYGNSS) and NDVI, SPI3 and TWS for 2018 to 2019. (The values reported in the figure are the average values of each variable of the two years)

period. Conversely, TWS and NDVI detect the dry conditions later, depicting some shifts in the evolution when compared against SMAP and CYGNSS. Thus, SMAP and CYGNSS observations can be considered highly sensitive to short-term dry conditions. Additionally, the spatial maps depict similar patterns, except for SPI3 and TWS, and SMAP and CYGNSS perfectly capture the drought conditions over the period, as captured by GLDAS and NDVI.

### 3.3 Correlation to NDVI, SPI3 and TWS indicators

We further investigated the correlation to SPI3, NDVI, and TWS indicators using the Pearson correlation coefficient ( $r$ ) and probability values ( $p$ -values), which are summarized in Table 4. Figure 5 shows a positive slope for all cases, indicating a good linear relationship, except between CYGNSS and TWS. The correlations between SMAP and SPI3, and between SMAP and NDVI, are strong with  $r=0.84$  and  $r=0.93$ , respectively, while the correlation between SMAP and TWS is lower with  $r=0.47$ . The correlations between CYGNSS and SPI3, and between CYGNSS and NDVI, are strong with  $r=0.78$  and  $r=0.86$ , respectively, while it is low with TWS ( $r=0.56$ ). For both soil moisture datasets, their correlation with TWS is low. This could be due to the fact that TWS is less sensitive to short-term dry conditions. The delayed responses of TWS could be attributed to the hydrological connectivity of the region and local topography. Furthermore, the data

points ( $n=38$ ) representing the relationship between SMAP or CYGNSS and the drought indicators (SPI3, NDVI, TWS) show relatively less dispersion in the SMAP scatterplots than in the CYGNSS scatterplots. This suggests a stronger correlation between SMAP and the variables compared to CYGNSS with the variables. The  $p$ -values between SMAP or CYGNSS and the indicators are significant, indicating a statistically meaningful relationship. The good correlation between SMAP or CYGNSS and the drought indicators suggests they are sensitive to drought conditions, especially for short-term drought monitoring. Short-term drought refers to a weather pattern that results in a precipitation deficit lasting for a few weeks up to six months. Figure 6 shows the spatial patterns of dry and wet conditions from SMAP, CYGNSS, GLDAS, and the drought indicators (SPI3, NDVI, and TWS) from October 2018 to August 2019. All the variables capture the dry conditions features similarly when compared to each other, except for SPI3 and TWS. Overall, SMAP and CYGNSS are relatively more sensitive to drought conditions when comparing the spatial map patterns and the temporal evolution of the plots of the variables.

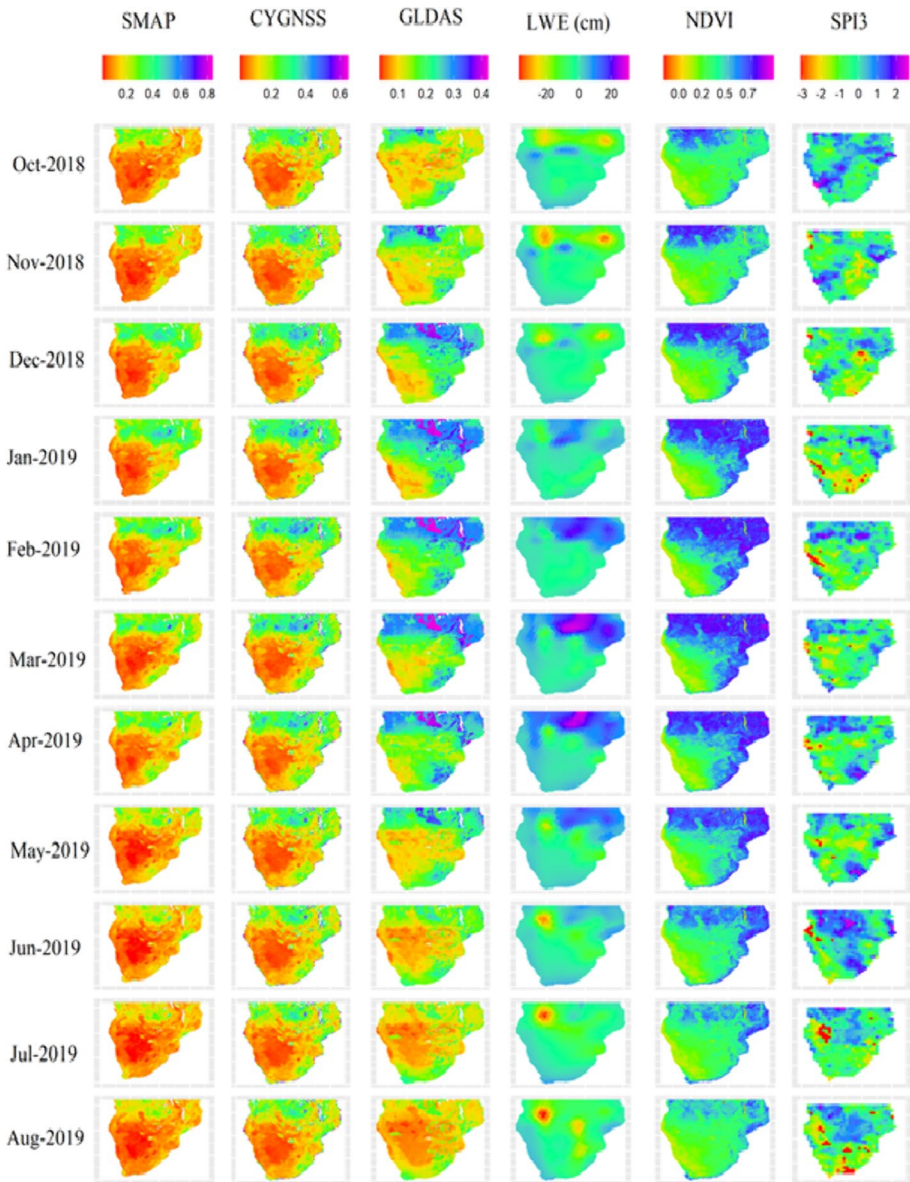
Our findings, as illustrated in Fig. 6, reveal that all variables displayed similar spatial patterns throughout the study period. The highest and lowest values varied according to each variable or indicator, denoting the drought classification. From October to December 2018, there was a consistent absence of drought. This began to escalate from January to March 2019, before experiencing a slight decline until September. The surge in January can be attributed to rainfall in late December, with a significant downpour occurring in February. Specifically, during the 2018–2019 year, there was a pronounced peak of rainfall in late December 2018 and above-average rainfall in the first week of February 2019.

Figure 7 presents the drought hotspots map of the Southern Africa region for the same period, computed using variables such as monthly rainfall, maximum dry spell in the month, start date of the growing season, and monthly averages of NDVI and Land Surface Temperature. Globally, the drought appears to be more severe in the southwest than in other regions, as depicted by both our computed spatial maps and the drought hotspots map. Overall, SMAP and CYGNSS observations accurately capture the drought and display very similar spatial patterns when compared with the drought hotspots map.

## 4 Discussion

Our assessment analysis reveals that SMAP and CYGNSS data have a strong correlation ( $r=0.98$  and  $r=0.97$  respectively) with GLDAS data for the study period, indicating their good accuracy and reliability. The correlations of SMAP to NDVI, SPI3, and TWS are  $r=0.93$ ,  $r=0.84$ , and  $r=0.47$ , respectively, while the correlations between CYGNSS and the same indicators are  $r=0.86$ ,  $r=0.78$ , and  $r=0.56$ , respectively.

The GLDAS model appears to detect drought conditions earlier than SMAP and CYGNSS (see Fig. 3). This may be due to the vegetation effect on the measurement since dense vegetation canopies are difficult to penetrate by the SMAP L-band (Chan et al. 2016) and significantly affect GNSS-R signals, leading to less sensitivity in changes in drought intensity. Due to rainfall that usually occurs in that period (December–February), the NDVI values are high consequently since there is a strong correlation between spatial and temporal patterns of NDVI and rainfall (Davenport et al. 1993). For the year 2018–2019 especially, the rainfall got a high peak in late December 2018 ([https://reliefweb.int/sites/reliefweb.int/files/resources/ca3071en\\_0.pdf](https://reliefweb.int/sites/reliefweb.int/files/resources/ca3071en_0.pdf)) and was heavier than average in the first week of February



**Fig. 6** Spatial distribution of dry and wet conditions of the indicators at the drought time span (drought occurred between October 2018 and August 2019). (The values reported in the maps are the average values of each variable of the two years)

2019 (<https://reliefweb.int/sites/reliefweb.int/files/resources/GlobalWeatherHazard19.02.15.pdf>).

In Fig. 4, the variables exhibit, overall, similar trends and patterns globally. Dry and wet conditions monitored through SMAP and CYGNSS agree, globally, with the low and high values in common areas of indices and rainfall events, except with SPI3, which

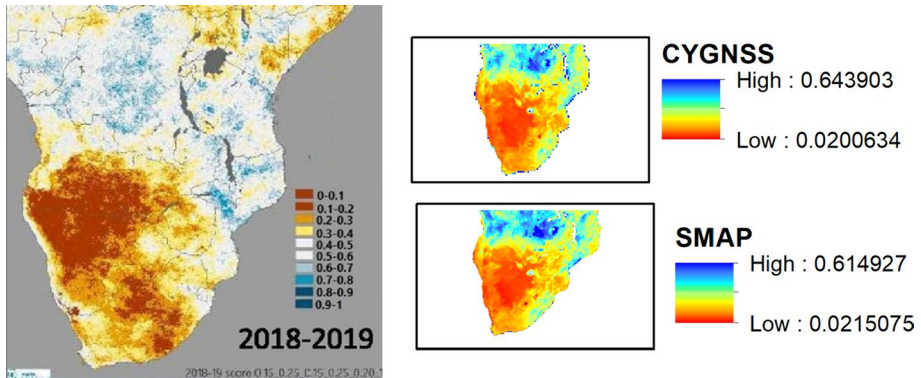


**Fig. 7** SMAP and CYGNSS soil moisture maps and reference map of drought spatial distribution of Southern Africa of the year 2018–2019 (“FAO in the 2019 humanitarian appeal: 2018/19 El Niño Response Plan for Southern Africa—Zimbabwe”. ReliefWeb)

presents a somewhat different trend in the first period, and with TWS and NDVI, which detect the dry conditions late. The SPI3 index has the potential for short-term resolution, but specifically, for seasonal drought monitoring, while the TWS is good for long-term periods. Thus, TWS could not detect the immediate impact of rainfall deficits on groundwater storage. The minor delay observed in NDVI to detect the dry conditions could be explained by the rainfall effects since it got a high peak in December.

Figure 7 presents the drought map for Southern Africa for the year 2018–2019, which serves as the reference drought map for validating the spatial distribution of wet and dry conditions of the drought indicators (as shown in Fig. 6). The data used to estimate the drought that affected Southern Africa during the periods 2015–2016 and 2018–2019 (ongoing) included monthly rainfall, maximum dry spell in the month, start date of the growing season, and monthly averages of NDVI and Land Surface Temperature. The output is presented as an anomaly of the standardized variable (“FAO in the 2019 humanitarian appeal: 2018/19 El Niño Response Plan for Southern Africa -Zimbabwe”. ReliefWeb). The comparison between the reference drought map and the computed maps of wet and dry conditions reveals a similar spatial distribution, thereby demonstrating the effectiveness of our analyses and results.

In other regions, a comparison of SMAP and the China Land Soil Moisture Data Assimilation System (CLSMDAS) for drought monitoring on a weekly basis was conducted by Qian Zhu et al. (2019). The authors found a correlation coefficient ( $r$ ) of 0.70, demonstrating that SMAP data is a good candidate for drought monitoring. Drought monitoring from satellite sensors offers many advantages such as global coverage, allowing for large area sensing, and daily revisiting time to monitor the onset of drought-related events, among others. The SMAP L-band enables all-weather conditions (cloud-penetrating), and soil moisture observations are possible under sparse and moderate vegetation, unlike other visible/near-infrared sensors. SMAP measurements are possible at day and night since these are independent of solar illumination (Velpuri et al. 2016). However, some limitations are encountered when estimating these soil moistures. Among them are uncertainties or unavailability of soil moisture over regions with dense vegetation, coarse resolution (36 km), and the need for in-situ data for validation purposes (Velpuri et al. 2016). One major disadvantage in using satellite data for

drought monitoring is that the spatial resolution is too large (e.g., SMAP  $\approx 3 \text{ km} \times 3 \text{ km}$ ,  $9 \text{ km} \times 9 \text{ km}$ , or  $36 \times 36 \text{ km}$ ) (Crow et al. 2012).

GNSS-R technology provides a high temporal and spatial resolution alternative method. Although there are still some remaining uncertainties and issues, soil moisture is one of the most important application fields for this technology. Some of the current problems and challenges in the space-borne GNSS-R soil moisture retrieval include polarization, coherent and non-coherent scattering components, observation geometry (Scattering Zenith angle and Azimuth angle), Brewster angle, Surface roughness, Vegetation Optical Depth (VOD), data dependence in the inversion algorithm, Effective Isotropic Radiated Power (EIRP), and Radio Frequency Interference (RFI). To reduce the polarization loss and improve the reception of the reflected signal, the antenna with the corresponding polarization should be used and the receiver needs a complex technical design (Wu et al., 2020). Moreover, the coherent and incoherent scattered energy of CYGNSS processing is currently a concern. Considering the incident signal is entirely a specular coherent scattering seems to be impossible since the actual surface is rough and if so, then there might be parts of diffuse scattering energy (Wu et al. 2021a, b). With a good spatio-temporal resolution, the GNSS-R consistent amount of data can be increased only if the effects of extreme incidence angles are considered. In fact, the reflection coefficient or bistatic scattering coefficient is highly affected by the angle information according to the observation geometries. However, in previous works, it is considered by some authors (Chew et al. 2018) while not taken into account in other studies (Kim et al. 2018). Surface roughness and the soil permittivity are highly paired making it difficult to differentiate the one, which influences the GNSS-R signal. However, surface roughness needs to be eliminated in the inversion for improving the retrieval accuracy. Vegetation effects on the incident GNSS signals and the reflected signals need to be removed since they change the scattering properties at different observation angles. To remove its effect during the inversion, the attenuation due to VOD is assumed to be constant even at different angles (Al-Khaldi et al. 2019), which appears to be too simple. For GNSS-R soil moisture retrieval by employing linear regression method, GNSS-R reflectivity, SMAP, VOD, and roughness coefficient are used in some studies making the inversion algorithm very dependent on ancillary data (Calabia et al. 2019, Chew et al. 2018). GNSS-R reflectivity data is affected by data calibration which has effects on the soil moisture retrieval (Molina et al. 2022), even though, this issue can be solved by EIRP method (Wu et al. 2021a, b). Radio Frequency Interference (RFI) can impact GNSS-R sensors through reflection, diffraction, atmospheric refraction, and scattering, and can be responsible for an unusual increase in reflected signals. However, to date, limited research on RFI for CYGNSS has been conducted (Wu et al. 2021a, b). GNSS-R offers numerous advantages such as global scale observation, very low revisit time, low cost, low power consumption, lightweight and small payloads, and near real-time massive data availability. However, a discrepancy can be noticed when comparing the estimated GNSS-R surface reflectivity values with the actual surface reflectivity values (Molina et al. 2022). Vegetation Optical Depth (VOD) estimates from optical remote sensing have been proposed and employed in many studies, and less dependence on SMAP and other ancillary data should be considered in future researches.

In summary, the soil moisture data from SMAP and CYGNSS are highly effective for drought monitoring and detection. This is particularly true in regions where data is scarce and for large-scale soil moisture monitoring, as these datasets offer significant advantages over traditional methods for estimating soil moisture. Both SMAP and CYGNSS data boast relatively high accuracy and provide global coverage with a high spatiotemporal resolution. This makes them invaluable tools in the field of drought monitoring.

However, although satellite soil moisture data has been used as a common approach to monitor and predict drought, it may not offer sufficiently accurate spatial outputs. In addition, different sensors have different algorithms with their advantages and disadvantages over different geographical and climate regions. For example, satellite soil moisture measurement over open water might lead to significant bias (Wu et al. 2016). Vegetation optical depth and surface roughness are among the parameters that most affect the signals and influence the data accuracy, especially for CYGNSS. Factors such as soil roughness and vegetation can significantly impact the accuracy of soil moisture estimates, and effectively mitigating these effects can yield highly reliable observation data at a high temporal and spatial resolution. In this study, the seasonal cycle effect was addressed using the Deseason function of Matlab, as outlined in the data analysis section. As for the effects of surface roughness and Vegetation Optical Depth (VOD), these were not considered during the computations due to their complexity and the extensive work required to address them. These factors could be the focus of a separate investigation. Making corrections to satellite soil moisture data to minimize the effects of these parameters would require a number of algorithms and additional data. Another limitation is the approximate threshold value of the soil moisture from which drought conditions can start and the corresponding drought classes.

Soil moisture plays an important role in drought monitoring and prediction, flood forecasting, landslide and soil erosion prediction and forest fire prediction. However, due to its complex relationship with different variables, the methodology used in this work focuses on drought monitoring (agricultural drought) even though it can be applied to other areas.

## 5 Conclusions

This study advocates for the use of soil moisture data as a direct tool for detecting droughts, particularly for short-term drought detection and monitoring. Soil moisture data from SMAP and CYGNSS have demonstrated strong correlations and good Root Mean Square Error (RMSE) values with GLDAS data. The validation of SMAP and CYGNSS soil moisture using GLDAS data as a reference value underscores the effectiveness of these satellite-based techniques in soil moisture monitoring. SMAP and CYGNSS soil moisture can provide drought detection, particularly for short-term drought events. This is confirmed by the strong correlation ( $r$ ) with drought indicators such as NDVI, SPI3, and TWS. We have demonstrated that SMAP and CYGNSS soil moisture can detect early drought conditions and provide short-term warnings. Thus, SMAP and CYGNSS soil moisture can deliver accurate short-term drought warnings, and have the advantage of being simple and easy to implement in practical applications for users such as farmers and government officials.

The direct use of soil moisture data for monitoring drought has numerous advantages, including its ease of use, simple computation, and no requirement for advanced data processing skills. In fact, utilizing soil moisture data to study and monitor drought is straightforward and accessible for the authorities responsible for this area. It allows for quick analysis of soil moisture changes and the ability to use those results to detect drought. Complex computations such as the Standardized Soil Moisture Index (SSI), Soil Water Index (SWI), Soil Moisture Anomaly (SMA), or Soil Water Deficit Index (SWDI) relatively require extensive data and are cumbersome. Utilizing direct measurement data may provide more accurate and beneficial results than derived data, especially when considering potential data alterations. However, it is important to be aware of the

seasonal cycle effect, which can impact the values of the time series and needs to be addressed during the study. Removing this effect is crucial to avoid its impact on trends, as non-stationarity in the data can lead to false correlations.

However, to ensure the reliability and effectiveness of our results, we used the Global Land Data Assimilation System (GLDAS) soil moisture data as a reference or ground truth for comparison and validation. This approach allowed us to confidently assess the accuracy of our soil moisture estimates, despite not accounting for surface roughness and VOD effects. To improve our ability to monitor drought and forecast its impacts at different spatio-temporal scales, reliable and accurate remote sensing techniques are essential. These methods can provide soil moisture measurements at a high spatial and temporal resolution, making them an effective supplement to existing observational methods.

This study underscores the potential and reliability of utilizing soil moisture data from SMAP and CYGNSS directly for drought monitoring, thereby enhancing existing methods and procedures. However, it is important to note that this study was confined to using soil moisture data only from 2018 to 2019 to demonstrate the effectiveness of this approach. For a more comprehensive evaluation and generalization of the results, it would be necessary to use more extensive data over a longer time period. Therefore, our method can be seen as a supplementary analysis to existing methods, rather than a replacement. Additional studies that employ multi-year time series data at different scales are needed to improve our understanding of changes in soil moisture and reveal the relationship between soil moisture evolution and drought severity. To achieve this, further research could involve generating correlation and slope maps between the indicators to detect their spatial strength, and examining the effects of geographical parameters such as vegetation, water bodies, urban areas, and terrain on their relationship. Achieving this would require data corrections as the first step.

**Authors' contributions** Data curation, K.E.; funding acquisition, S.J.; methodology, K.E., S.J. and I.M.; computation, K.E. and U.M.; supervision, S.J. and I.M.; writing—original draft, K.E.; writing—review and editing, S.J., I.M., A.C. and I.U. All authors have read and agreed to the published version of the manuscript.

**Funding** Financial supports of this work were provided by Shanghai Leading Talent Project (Grant No. E056061).

## Declarations

**Competing interests** All the authors declare that they have no conflict of interests.

**Consent to participate** Consents for participation from all the co-authors are received.

**Consent to publish** Consents for publication from all the co-authors are received.

## References

- AghaKouchak A (2014) A baseline probabilistic drought forecasting framework using Standardized Soil Moisture Index: application to the 2012 United States drought. *Hydrol Earth Syst Sci* 18(7):2485–2492. <https://doi.org/10.5194/hess-18-2485-2014>
- AghaKouchak A, Nakhjiri N (2012) A near real-time satellite-based global drought climate data record. *Environ Res Lett* 7(4):044037. <https://doi.org/10.1088/1748-9326/7/4/044037>

- AghaKouchak A, Farahmand A, Melton FS, Teixeira J, Anderson MC, Wardlow BD, Hain CR (2015) Remote sensing of drought: progress, challenges and opportunities. *Rev Geophys* 53:452–480. <https://doi.org/10.1002/2014RG000456>
- Al-Khaldi MM, Johnson JT, O'Brien AJ, Balenzano A, Mattia F (2019) Time-series retrieval of soil moisture using CYGNSS. *IEEE Trans Geosci Remote Sens* 57(7):4322–4331
- Anderson MC, Hain C, Wardlow B, Pimstein A, Mecikalski JR, Kustas WP (2011) Evaluation of drought indices based on thermal remote sensing of evapotranspiration over the continental United States. *J Clim* 24(8):2025–2044. <https://doi.org/10.1175/2010JCLI3812.1>
- Bai et al (2018) Assessment of the SMAP-derived soil water deficit index (SWDI-SMAP) as an agricultural drought index in China. *Remote Sens* 10(8):1302. <https://doi.org/10.3390/rs10081302>
- Beguieria S, Vicente-Serrano SM, Reig F, Latorre B (2014) Standardized precipitation evapotranspiration index (SPEI) revisited: parameter fitting, evapotranspiration models, tools, datasets and drought monitoring. *Int J Climatol* 34:3001–3023
- Bittelli M, Valentino R, Salvatorelli F, Rossi Pisa P (2012) Monitoring soil-water and displacement conditions leading to landslide occurrence in partially saturated clays. *Geomorphology* 173–174:161–173
- Bolten JD, Crow WT, Zhan X, Jackson TJ, Reynolds CA (2010) Evaluating the utility of remotely sensed soil moisture retrievals for operational agricultural drought monitoring. *IEEE J Sel Top Appl Earth Obs Remote Sens* 3(1):57–66. <https://doi.org/10.1109/JSTARS.2009.2037163>
- Brocca L, Melone F, Moramarco T, Wagner W, Naeimi V, Bartalis Z, Hasenauer S (2010) Improving runoff prediction through the assimilation of the ASCAT soil moisture product. *Hydrol Earth Syst Sci* 14:1881–1893
- Brocca L, Ponziani F, Moramarco T, Melone F, Berni N, Wagner W (2012) Improving landslide forecasting using ASCAT-derived soil moisture data: a case study of the Torgiovannetto landslide in central Italy. *Remote Sens* 4:1232–1244
- Calabia A, Molina I, Jin SG (2019) Soil moisture content from GNSS reflectometry using dielectric permittivity from fresnel reflection coefficients. *Remote Sens* 12(1):122. <https://doi.org/10.3390/rs12010122>
- Chan S, Bindlish R, O'Neill PE, Njoku E, Jackson T, Colliander A, Chen F, Burgin M, Dunbar S, Piepmeier J et al (2016) Assessment of the SMAP passive soil moisture product. *IEEE Trans Geosci Remote Sens* 54:1–14
- Chew CC, Small EE (2018) Soil moisture sensing using spaceborne GNSS reflections: comparison of CYGNSS reflectivity to SMAP soil moisture. *Geophys Res Lett* 45(9):4049–4057
- Crow W T, Berg A A, Cosh M H, Loew A, Mohanty B P, Panciera R, Rosnay P, Ryu D, Walker J P (2012) Upscaling sparse ground-based soil moisture observations for the validation of coarse-resolution satellite soil moisture products. *Rev Geophys* 50
- Davenport ML, S E NICHOLSON, (1993) On the relation between rainfall and the normalized difference vegetation index for diverse vegetation types in East Africa. *Int J Remote Sens* 14(12):2369–2389. <https://doi.org/10.1080/01431169308954042>
- Easterling D (2013) Global data sets for analysis of climate extremes. *Extrem Changing Clim* 65:347–361. <https://doi.org/10.1007/978-94-007-4479-012>
- Edokossi et al (2020) GNSS-reflectometry and remote sensing of soil moisture: a review of measurement techniques, methods, and applications. *Remote Sens* 12:614. <https://doi.org/10.3390/rs12040614>
- Enekel M, Steiner C, Mistelbauer T, Dorigo W, Wagner W, See L, Atzberger C, Schneider S, Rogenhofer E (2016) A combined satellite-derived drought indicator to support humanitarian aid organizations. *Remote Sens* 8:340
- Entekhabi D et al (2004) The hydrosphere state (Hydros) satellite mission: an earth system pathfinder for global mapping of soil moisture and land freeze/thaw. *IEEE Trans Geosci Remote Sens* 42(10):2184–2195. <https://doi.org/10.1109/TGRS.2004.834631>
- Entekhabi D et al (2010) The soil moisture active passive (SMAP) mission. *Proc IEEE* 98(5):704–716. <https://doi.org/10.1109/JPROC.2010.2043918>
- Eswar R, Das NN, Poulsen C, Behrangi A, Swigart J, Svoboda M, Entekhabi D, Yueh S, Doorn B, Entin J (2018) SMAP Soil Moisture Change as an Indicator of Drought Conditions. *Remote Sens* 10(5). <https://doi.org/10.3390/rs10050788>
- Field CB (2012) Managing the risks of extreme events and disasters to advance climate change adaptation: special report of the intergovernmental panel on climate change. Cambridge University Press, Cambridge, p 2012
- Forootan E et al (2019) Understanding the global hydrological droughts of 2003–2016 and their relationships with teleconnections. *Sci Total Environ* 650:2587–2604. <https://doi.org/10.1016/j.scitotenv.2018.09.231>
- Gebrehiwot T et al (2011) Spatial and temporal assessment of drought in the Northern highlands of Ethiopia. *Int J Appl Earth Observ Geoinform* 13(3):309–321. <https://doi.org/10.1016/j.jag.2010.12.002>

- Gleason S, Adjrard M Sensing ocean, ice and land reflected signals from space: results from the UK-DMC GPS reflectometry experiment (2005) In: Proceedings of the 18th international technical meeting of the satellite division of the institute of navigation, Long Beach, CA, USA, 13–16 Sept 2005
- Godfray HC, Beddington JR, Crute IR, Haddad L, Lawrence D, Muir JF, Pretty J, Robinson S, Thomas SM, Toulmin C (2010) Food security: the challenge of feeding 9 billion people. *Science* 327(5967):812–818. <https://doi.org/10.1126/science.1185383>
- Hao Z, AghaKouchak A (2013) Multivariate standardized drought index: a parametric multi-index model. *Adv Water Res* 57:12–18. <https://doi.org/10.1016/j.advwatres.2013.03.009>
- Hofmann-Wellenhof B, Lichtenegger H, Wasle E (2008) GNSS-global navigation satellite systems: GPS, GLONASS, Galileo and More, 1st edn. Springer, Wien, p 518
- Ji L, Peters AJ (2003) Assessing vegetation response to drought in the northern great plains using vegetation and drought indices. *Remote Sens Environ* 87(1):85–98. [https://doi.org/10.1016/S0034-4257\(03\)00174-3](https://doi.org/10.1016/S0034-4257(03)00174-3)
- Jia Y, Savi P (2017) Sensing soil moisture and vegetation using GNSS-R polarimetric measurement. *Adv Space Res* 59:858–869
- Jin S, Komjathy A (2010) GNSS reflectometry and remote sensing: new objectives and results. *Adv Space Res* 46:111–117
- Kim J, Hogue T (2012) Improving spatial soil moisture representation through integration of AMSR-E and MODIS products. *IEEE Trans Geosci Remote Sens* 50(2):446–460
- Kim H, Lakshmi V (2018) Use of cyclone global navigation satellite system (CyGNSS) observations for estimation of soil moisture. *Geophys Res Lett* 45:8272–8282
- Kongoli C, P Romanov, R Ferraro (2012) Snow cover monitoring from remote sensing satellites. In: Remote sensing of drought: innovative monitoring approaches, pp. 359–386, CRC Press
- Koster RD, Mahanama SPP, Livneh B, Lettenmaier D, Reichle RH (2010) Skill in streamflow forecasts derived from large-scale estimates of soil moisture and snow. *Nat Geosci* 3:613–616
- Lawal S, Lennard C, Hewitson B (2019) Response of southern African vegetation to climate change at 1.5 and 2.0 global warming above the pre-industrial level. *Clim Serv* 16:100134
- Molina I, Calabia A, Jin S, Edokossi K, Wu X (2022) Calibration and validation of CYGNSS reflectivity through wetlands' and deserts' dielectric permittivity and validation with SMAP data. *Remote Sens* 14:3262. <https://doi.org/10.3390/rs14143262>
- Njoku EG, Jackson TJ, Lakshmi V, Chan TK, Nghiem SV (2003) Soil moisture retrieval from AMSR-E. *IEEE Trans Geosci Remote Sens* 41(2):215–229. <https://doi.org/10.1109/TGRS.2002.808243>
- Parry M, Canziani OF, Palutikof JP, van der Linden PJ, Hanson CE (2007) Climate change, 2007 impacts, adaptation and vulnerability. Cambridge University Press, Cambridge, p 4
- Rahmani A, Golian S, Brocca L (2016) Multiyear monitoring of soil moisture over Iran through satellite and reanalysis soil moisture products. *Int J Appl Earth Obs Geoinf* 48:85–95
- Raziei T, Saghaifan B, Paulo AA et al (2009) Spatial patterns and temporal variability of drought in western Iran. *Water Resour Manag* 23:439–455. <https://doi.org/10.1007/s11269-008-9282-4>
- Reichle RH, Koster RD, Dong J, Berg AA (2004) Global soil moisture from satellite observations, land surface models, and ground data: implications for data assimilation. *J Hydrometeorol* 5(3):430–442
- Rodell M, Famiglietti J (2002) The potential for satellite-based monitoring of groundwater storage changes using GRACE: The high plains aquifer, central US. *J Hydrol* 263(1):245–256
- Rossi S, Niemeier S (2012) Drought monitoring with estimates of the fraction of absorbed photosynthetically-active radiation (fAPAR) derived from MERIS. In: Wardlaw B, Anderson M, Verdin J (eds) Remote sensing for drought: innovative monitoring approaches. CRC Press, Boca Raton, pp 95–116
- Sánchez N, González-Zamora Á, Piles M, Martínez-Fernández J (2016) A new soil moisture agricultural drought index (SMADI) integrating MODIS and SMOS products: a case of study over the Iberian Peninsula. *Remote Sens* 8:287
- Seager R, Hoerling M, Schubert S, Wang H, Lyon B, Kumar A, Nakamura J, Henderson N (2015) Causes of the 2011–14 California drought. *J Clim* 28(18):6997–7024. <https://doi.org/10.1175/JCLI-D-14-00860.1>
- Sheffield J, Goteti G, Wen F, Wood E (2004) A simulated soil moisture-based drought analysis for the United States. *J Geophys Res* 109:D24108. <https://doi.org/10.1029/2004JD005182>
- Sheffield J, Wood E, Roderick M (2012) Little change in global drought over the past 60 years. *Nature* 491(7424):435–438
- Singh H, Thompson A (2016) Effect of antecedent soil moisture content on soil critical shear stress in agricultural watersheds. *Geoderma* 262:165–173
- Sorooshian S et al (2011) Advanced concepts on remote sensing of precipitation at multiple scales. *Bull Am Meteorol Soc* 92(10):1353–1357

- Takada M, Mishima Y, Natsume S (2009) Estimation of surface soil properties in peatland using ALOS/PALSAR. *Landscape Ecol Eng* 5(1):45–58
- Velpuri NM, Senay GB, Morisette JT (2016) Evaluating new SMAP Soil moisture for drought monitoring in the rangelands of the US high plains. *Rangelands* 38(4):183–190. <https://doi.org/10.1016/j.rala.2016.06.002>
- Vicente-Serrano SM, López-Moreno JI (2005) Hydrological response to different time scales of climatological drought: an evaluation of the Standardized Precipitation Index in a mountainous Mediterranean basin. *Hydrol Earth Syst Sci* 9(5):523–533
- Vicente-Serrano SM, Beguería S, López-Moreno JI (2010) A multiscalar drought index sensitive to global warming: the standardized precipitation evapotranspiration index. *J Clim* 23:1696–1718
- Wagner W, Dorigo W, de Jeu R, Fernandez D, Benveniste J, Haas E, Ertl M (2012) Fusion of active and passive microwave observations to create an essential climate variable data record on soil moisture. *ISPRS annals of the photogrammetry, remote sensing and spatial information sciences*, 1. <https://doi.org/10.5194/isprsannals-I-7-315-2012>
- Wang L, Qu JJ (2009) Satellite remote sensing applications for surface soil moisture monitoring: a review. *Front Earth Sci Chin* 3(2):237–247
- Wu XR, Jin SG (2020) Models and theoretical analysis of SoOP circular polarization bistatic scattering for random rough surfaces. *Remote Sens* 12:1506
- Wu Q, Liu H, Wang L, Deng C (2016) Evaluation of AMSR2 soil moisture products over the contiguous United States using in situ data from the International soil moisture network. *Int J Appl Earth Obs Geoinf* 45:187–199
- Wu X, Song Y, Xu J, Duan Z, Jin SG (2021a) Bistatic scattering simulations of circular and linear polarizations over land surface for signals of opportunity reflectometry. *Geosci Lett* 8:11. <https://doi.org/10.1186/s40562-021-00182-y>
- Wu X, Ma W, Xia J, Bai W, Jin S, Calabria A (2021b) Spaceborne GNSS-R soilmoisture retrieval: status, development opportunities, and challenges. *Remote Sens* 13:45. <https://doi.org/10.3390/rs13010045>
- Zhu Q, Luo Y, Yue-Ping Xu, Tian Ye, Yang T (2019) Satellite soil moisture for agricultural drought monitoring: assessment of SMAP-derived soilwater deficit index in Xiang river basin. *China Remote Sens* 11:362. <https://doi.org/10.3390/rs11030362>

**Publisher's Note** Springer Nature remains neutral with regard to jurisdictional claims in published maps and institutional affiliations.

Springer Nature or its licensor (e.g. a society or other partner) holds exclusive rights to this article under a publishing agreement with the author(s) or other rightsholder(s); author self-archiving of the accepted manuscript version of this article is solely governed by the terms of such publishing agreement and applicable law.

## Authors and Affiliations

Komi Edokossi<sup>1</sup>  · Shuanggen Jin<sup>1,2</sup> · Usman Mazhar<sup>1</sup> · Iñigo Molina<sup>1,3</sup> · Andres Calabria<sup>4</sup> · Irfan Ullah<sup>5,6</sup>

✉ Shuanggen Jin  
sgjin@nuist.edu.cn; sg.jin@yahoo.com

Komi Edokossi  
ametokomi@gmail.com

Usman Mazhar  
usmanmazhargeo@outlook.com

Iñigo Molina  
inigo.molina@upm.es

Andres Calabria  
andres@calabria.com

Irfan Ullah  
irfan.marwat@nuist.edu.cn

- <sup>1</sup> School of Remote Sensing and Geomatics Engineering, Nanjing University of Information Science and Technology, Nanjing 210044, China
- <sup>2</sup> Shanghai Astronomical Observatory, Chinese Academy of Sciences, Shanghai 200030, China
- <sup>3</sup> School of Land Surveying, Geodesy and Mapping Engineering, Universidad Politécnica de Madrid, South Campus, 28031 Madrid, Spain
- <sup>4</sup> Department of Physics and Mathematics, University of Alcalá, Alcalá de Henares, Spain
- <sup>5</sup> School of Atmospheric Science, Nanjing University of Information Science and Technology, Nanjing 210044, China
- <sup>6</sup> Key Laboratory of Meteorological Disaster, Ministry of Education/Joint International Research Laboratory of Climate and Environment Change/Collaborative Innovation Centre On Forecast and Evaluation of Meteorological Disasters, Nanjing University of Information Science and Technology, Nanjing, China